Polydispersity and structure: a qualitative comparison between simulations and granular systems data

R. Sánchez, I. C. Romero-Sánchez, S. Santos-Toledano and A. Huerta
Departamento de Física, Facultad de Física e Inteligencia Artificial, Universidad Veracruzana, Circuito Gonzalo Aguirre Beltrán s/n, Zona Universitaria, Xalapa 91000, Veracruz, Mexico.

Received 22 August 2013; accepted 7 January 2014

Various quasi-2D systems are examined experimentally, particularly via the radial distribution function, in an inexpensive and convenient driven granular system. Results regarding the effects of polydispersity and granular collapse are presented. It is found that, even using a simple size distribution, Monte Carlo equilibrium simulations can successfully reproduce the experimental results with only minor corrections arising from observed granular collapse, and that polydispersity of ~ 7 % suppresses crystallization.

Keywords: Quasi-2D; granular collapse; jamming; driven granular media.

PACS: 68.18.-g; 68.47.Pe; 81.05.Rm; 64.70.P-

1. Introduction

Quasi-2D systems are those in which 3D constituents are constrained, by walls or external potentials, to move largely along a plane. Granular quasi-2D systems have been studied experimentally before (see, for example, Reis *et al.* [1] or Pacheco-Vázquez *et al.* [2]), but a particularly inexpensive yet useful model experimental system is presented here. The present work focuses on polydispersity effects, although even for monodisperse hard disks, which have long been studied, the precise caging mechanism driving crystallization remains controversial [3].

Experimental results [5,6] suggest that hard-sphere behavior occurs in quasi-2D colloidal systems that, due to the presence of electric charges, cannot be assumed *a priori* to be hard spheres. In addition, other repulsive systems such as Yukawa disks exhibit similarities in their freezing transitions to those of hard disks [7].

With relatively few exceptions, such as the work of Wang *et al.* [8], most experimental quasi-2D work has focused on near-monodisperse particles rather than examining the effects of polydispersity, particularly in systems exhibiting any form of granular collapse (as defined by Tobochnik [9], the loss of nearly all kinetic energy due to inelastic collisions), and thus further experimental evidence is needed to elucidate the polydispersity conditions under which crystallization will occur, especially in systems not in thermodynamic equilibrium. In addition, colloidal size distributions, for example, are often non-trivial or asymmetric [10-12], further complicated in quasi-2D systems by the additional variation in collision distances along the plane introduced by collisions not wholly along the plane of motion, for which even monodisperse rigid spheres collide at varying center-to-center distances along the plane, an effect that has sometimes been treated as a soft potential [13]. Polydispersity can frustrate freezing in strictly 2D hard disks (see Fig. 4) and can suppress the split of the second peak of the radial distribution function. However, a bidisperse system [3], which also does not exhibit a freezing transition, still shows a split in the second oscillation in the radial distribution function, a feature originally attributed to the structural precursor of freezing [17]. Due to these complications, models capturing the true experimental behavior without relying on detailed emulation of specific experimental distributions and the characterization of non-trivial model systems are highly desirable. We seek to shed light on some of these issues using an inexpensive and convenient experimental setup with hard interactions.

The 2-dimensional radial distribution function $g(r)$ is defined as follows [4]:

$$g(r)dr = \frac{n(r)}{a(r)}\frac{A}{N}dr\,, \tag{1}$$

where r is the 2D distance from a known particle center along the plane of motion, dr, for experimental and simulational results, is a fixed bin size that is finite but small on the scale of the particles, $n(r)$ is the number of particle centers found between distances r and $r+dr$ from the origin (*i.e.*, the number of particle centers between concentric circles of radii r and $r+dr$ centered on a particle center), $a(r)$ is the area between concentric circles of radii r and $r+dr$, N is the total number of particles detected in the entire system and A is the total physical area available. In systems with significant finite size effects, and in inhomogeneous systems (those with temperature gradients, for example) $g(r)$ cannot be assumed *a priori* to tend to unity at large separations.

In the present work we present experimental and simulational results regarding the effects of polydispersity and granular collapse on a model system. Two experimental systems with granular collapse and different polydispersities are examined, and are compared to simulations involving polydispersity but without granular collapse.

2. Materials and Methods

In all cases, vibrations were applied by a speaker (Sony, 190 W peak output, 16 cm) driven by a 150 Hz sinusoidal

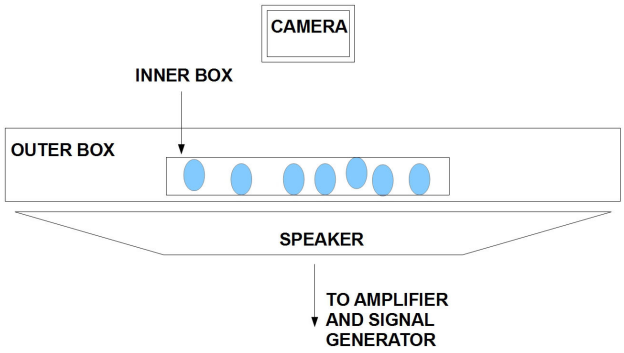

FIGURE 1. The experimental setup used is shown schematically. The filled circles indicate the particles used (not shown to scale). The inner box has dimensions 9.1×7.1 cm.

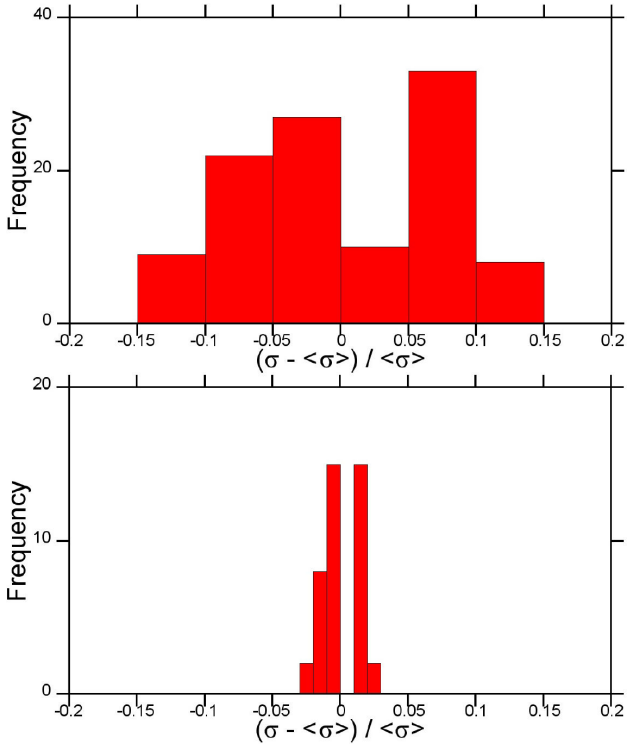

FIGURE 2. Size histograms of polydisperse polystyrene spheres (top) and near-monodisperse beads (bottom) are shown. While the distribution shapes are qualitatively similar, it is evident that the beads are far more monodisperse.

wave from a signal generator (Phillips PM5132) and an amplifier (Steren AMP-010, 35 W rms), as shown schematically in Fig. 1. Images were captured by a Microsoft LifeCam VX-800 webcam at a rate of 5 frames per second; using a rate over an order of magnitude slower than the driving frequency ensures non-negligible agitation between frames. Fundamentally, this system is reminiscent of that used, for example by Gradenigo *et al.* [14], but using a much more inexpensive apparatus. The following types of spherical particles were used at various packing fractions η: 0.35 mm mean diameter, 6.76 % polydispersity Styrofoam spheres, and 0.77 cm mean diameter near-monodisperse plastic beads (snapshots of both systems are shown in Fig. 3). Histograms of the measured

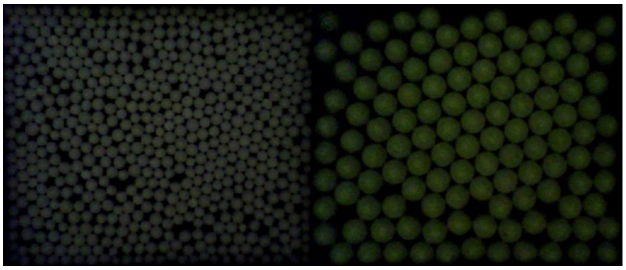

FIGURE 3. A snapshot of the near-monodisperse system at a packing fraction of 0.728 is shown on the left-hand side of the image, whereas on the right-hand side a snapshot of the polydisperse system at a packing fraction of 0.778 is shown. The image has been adjusted for brightness and contrast.

size distributions of the latter two are shown in Fig. 2. Conditions were chosen so that the systems remained quasi-2D. In the case of the solid plastic spheres, their greater weight reduces the effects of non-radial collisions. For the small Styrofoam particles, their low density could make hydrodynamic interactions non-negligible, emulating colloids in a fluid.

The obtained image sequences were analyzed using an ImageJ plugin developed by Sbalzarini and Koumoutsakos [15], which yields center coordinates as a function of frame number. The radial distribution functions for each set of coordinates were obtained by suitable code written in-house. To minimize distortions introduced by depletion due to lateral confinement, analysis of the plastic spheres and of the polydisperse Styrofoam spheres excluded centers detected within a mean diameter of the walls. In the case of polydisperse Styrofoam spheres, for all area fractions examined the number of particles per frame is ~ 500; for the near-monodisperse beads, ~ 100 were used and a greater number of frames was used to ensure good statistics.

The Monte Carlo (MC) simulations were of strictly 2-dimensional hard disks in equilibrium in the NVT ensemble, and periodic boundary conditions were used. Polydispersity was modeled as flat – a constant probability density between $\langle\sigma\rangle-\delta$ and $\langle\sigma\rangle+\delta$, and zero elsewhere. The absence of finite size effects was verified by varying the monodisperse system size (400 and 2500 particles), which had no significant effect on the results.

3. Results and Discussion

In Fig. 5, the particle positions in 200 frames from a single experiment using 100 near-monodisperse particles, and from another single experiment using 579 polydisperse particles, are shown. In the first case, near the center, an orderly, near-hexagonal arrangement can be seen; towards the figure's right-hand side, a less dense, disordered region, partially vacated by leftwards granular collapse can be seen. Near the remaining edges, finite size effects can be seen, as the boundary conditions (steric exclusion around hard walls) disrupt the hexagonal lattice, an effect that at separations comparable to

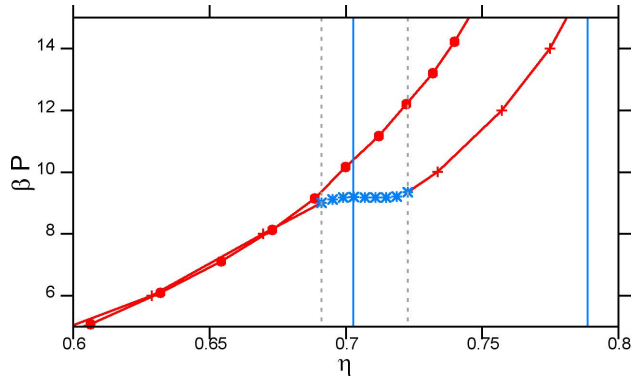

FIGURE 4. Monte Carlo (MC) equation of state of a polydisperse hard-disk flat distribution with δ=0.2 (filled circles) compared with a monodisperse strictly 2D hard-disk system (+), in terms of the normalized pressure βP and the packing fraction η. The dashed vertical lines indicate the packing fractions corresponding to freezing and melting points, η_f=0.69 and η_m=0.723, respectively, whereas the solid lines indicate the region in which most experiments were carried out. The region between the dashed lines is the fluid-solid transition region and the results depicted by asterisks are taken from the extensive MC simulations study by Mak [16]; the rest of the monodisperse disk data (+) are taken from MC simulations by Huerta *et al*. [17], and the data for polydisperse disks are novel MC results.

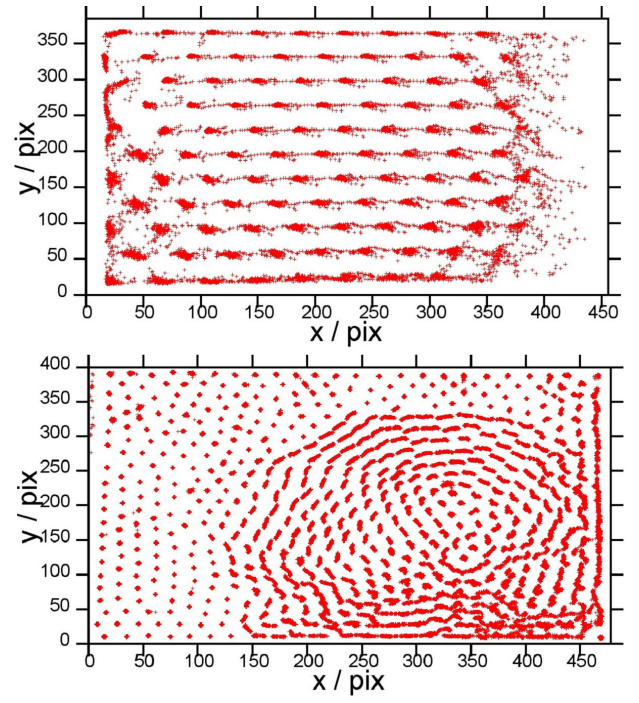

FIGURE 5. Positions of particle centers for a system of 100 near-monodisperse particles (η = 0.607), for 200 frames (top). Positions of particle centers for a system of 579 polydisperse particles (η = 0.789), again for 200 frames (bottom).

the box size becomes relevant to a significant fraction of the pairs considered for calculating $g(r)$. In the case of polydisperse particles, which are at a higher global packing fraction, it can be seen that granular collapse has caused the particles

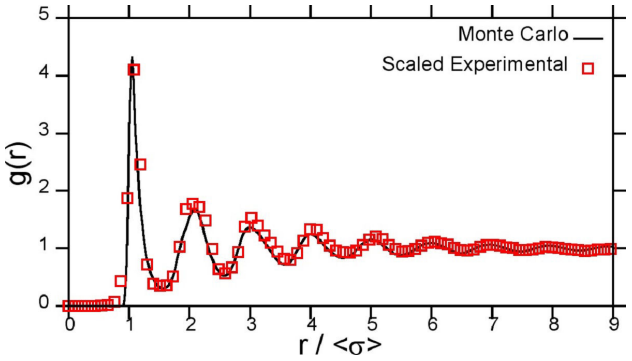

FIGURE 6. Radial distribution functions obtained at a packing fraction of 0.696, obtained from polydisperse (δ=0.07) strictly 2D MC simulations and experimentally from $\sim$ 7 % polydispersity spheres. For the experimental $g(r)$, the center-to-center distances have been scaled by a factor of 1.08 (see text).

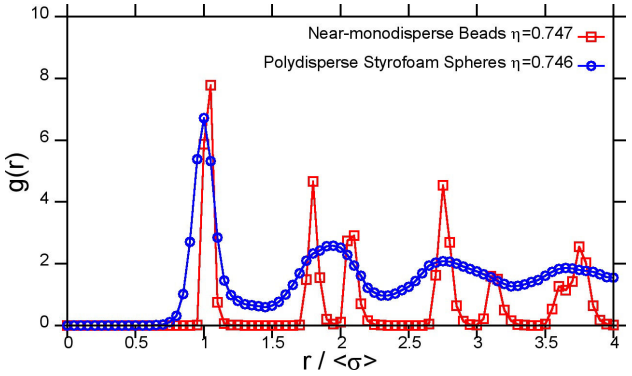

FIGURE 7. Radial distribution functions of near-monodisperse beads and $\sim$ 7 % polydispersity Styrofoam spheres at an area fraction of $\sim$ 0.75. Peak positions coincide, but the difference in sharpness is stark, particularly in terms of double peaks. Both systems are at packing fractions above the melting point (see Fig. 4).

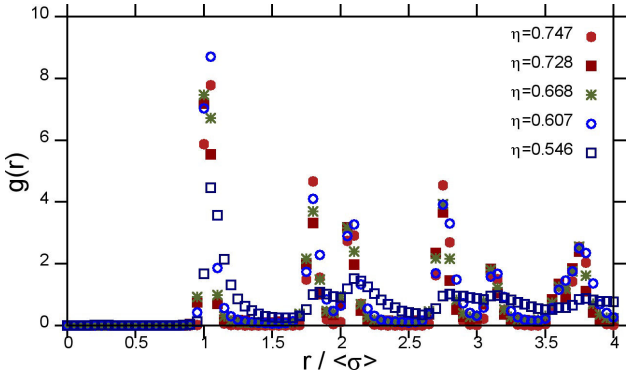

FIGURE 8. Radial distribution functions of near-monodisperse beads at packing fractions below, within and above the solid-fluid coexistence region for hard disks (see Fig. 4).

in left-hand side of the figure to arrange themselves into a locally highly packed cluster with little motion, while those near the lower left corner exhibit more fluid-like behavior.

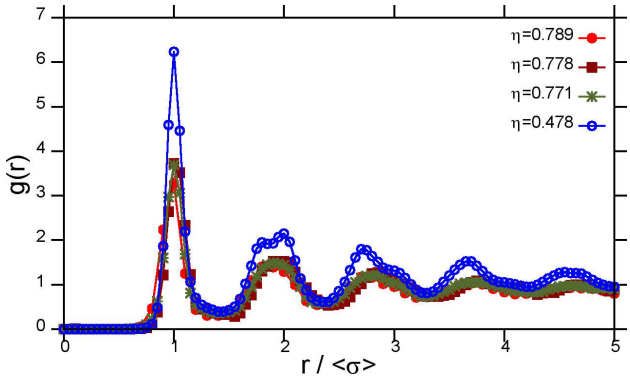

FIGURE 9. Radial distribution functions of ~ 7 % polydispersity Styrofoam spheres at various packing fractions.

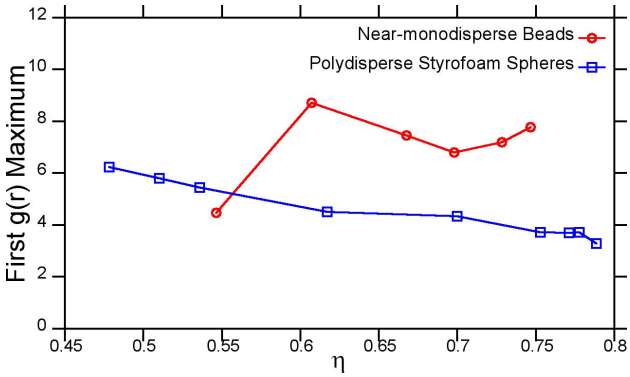

FIGURE 10. First maxima of the radial distribution functions of near-monodisperse beads and of ~ 7 % polydispersity Styrofoam spheres at various packing fractions. The values are non-monotonic functions of the packing fraction (see text).

The monodisperse plastic spheres have a radial distribution function that, as shown in Fig. 8, exhibits a clear split in the second peak, which is attributable not only to their low polydispersity, but also to their greater weight, resulting in a smaller vertical motion, in turn reducing the deviation of collisions from radial ones. This confirms the relationship between the split in the second peak and low overall variation in r at collision in the experimental system. It should be noted that near-zero local minima of $g(r)$ correspond to boundaries separating sharply defined layers of neighbors.

Care was taken to level the setup before conducting each experiment; nevertheless, it was observed that, particularly at low packing fractions, the particles tended to move in some particular direction. This can be explained on the basis of the speaker-driven agitation; the plane the particles can move in, being flat, is not equidistant to the speaker center, resulting in inhomogeneous oscillation amplitudes and thus inhomogeneous agitation. The box containing the particles was itself placed within another plastic box to reduce inhomogeneities, but they were not eliminated entirely. Inhomogeneous agitation is somewhat analogous to temperature gradients in colloidal and molecular systems and, as particles are driven into "cold," highly-packed regions, they lose nearly all their kinetic energy due to inelastic collisions, which is likely causing the experimental peaks to appear at somewhat lower separations than predicted computationally for homogeneous systems (see Fig. 6) and may be a contributing factor to $g(r)$ at large separations remaining somewhat below unity. Stationary states with spatial kinetic energy variations in granular systems are more poorly understood than systems emulating thermodynamic equilibrium, but the effects of such kinetic energy inhomogeneities in systems with inelastic collisions have been characterized in simulations by Tobochnik [9] as a granular collapse, which for the system studied led to a percolation transition. There remain important open questions regarding the effects of changes in the kinetic energy of granular systems, even for hard interactions [18].

Figure 7 compares $g(r)$ for near-monodisperse and polydisperse particles at very similar packing fractions. Peaks are found at essentially the same normalized separations, showing that the discrepancy with the computationally obtained positions in Fig. 6 is a feature of this experimental setup and not an artifact of the specific particles used for the results shown in that figure. The stark contrast between the soft polydisperse $g(r)$, with no hint of split peaks, and that of the more monodisperse system, whose split in the second peak falls to nearly zero illustrates the hindering of crystallization by polydispersity at these packing fractions; the combination of a liquid-like structure and no split in the second peak is consistent with frustration of the caging mechanism proposed by Huerta *et al.* [3]. Our results are also consistent with the MC simulations of polydisperse hard disks of Santen and Krauth [19], according to which crystallization is suppressed at polydispersities above ~ 0.1; once the effects of non-radial collisions are considered, the polydisperse spheres are likely to be in, or close to, this regime. The simulations of Kawasaki *et al.* [20] of polydisperse systems also predict comparable behavior. The small deviation from unity observed at large separations suggests finite size effects are modest and that thus comparing the experimental results with simulations using periodic boundary conditions is reasonable.

Counterintuitively, in Fig. 8 $g(r)$ exhibits a split second peak even at a packing fraction of 0.546, well below the MC coexistence region (see Fig. 4) and the first maximum is a non-monotonic function of the packing fraction, as shown in Fig. 10. The former feature can be explained as the result of inhomogeneous agitation driving granular collapse – most particles are driven into low-agitation, high local packing fraction regions (producing a locally highly packed, jammed region, the high density of which accounts for features such as the split double peak usually associated with highly packed systems). It is possible that this mechanism, dominant at low packing fractions, produces different peak heights than analogous states at high global packing fractions. A fall in the first peak's height past a certain packing fraction is a feature of the jamming transition in quasi-2D experimental colloidal systems with some overlap between the particles [21], which was explained as resulting from a wider first peak as the jammed states have a higher degree of particle overlap. While jamming in a dissipative system such as ours is not in

itself surprising, it is not obvious *a priori* that it should lead to features qualitatively similar to those of jamming in thermal systems.

The polydisperse system shows even more dramatic analogous effects – in Fig. 9, several radial distribution functions at packing fractions ~ 0.78 are comparable with the radial distribution function at a packing fraction of 0.478. The latter has a significantly higher first peak, generally sharper peaks, and its second peak exhibits a slight split, unlike the more liquid-like radial distributions at higher packing fractions. Granular collapse, for the less packed systems, appears to be a more effective crystallization mechanism than equilibrium-like caging at high global packing fractions. Consistent with the third and fourth peaks occurring at slightly lower separations for the less packed system, collapse dynamics may favor locally highly ordered arrangements into which at modest packing fractions the particles can more readily re-arrange themselves since their motion is less hindered, but understanding the role of these effects remains a theoretical and experimental challenge. Nevertheless, as Fig. 6 shows, simply scaling the separations by a factor close to unity yields excellent agreement between polydisperse strictly 2D MC simulations, which reproduce the key result that polydispersity suppresses both crystallization and the split in the second peak, and the experimental results; this scaling factor can be justified as the result of the typical experimental interparticle separations being reduced by granular collapse, since $g(r)$ at low separations is going to be dominated by the highly packed (and hence with separations dominated by contact) regions arising from granular collapse, whereas all the computational results assume spatially homogeneous conditions.

Emulating the detailed experimental dynamics would require more sophisticated computational models, but it is remarkable that the comparatively simple MC simulations used are in such good agreement with experiment, in terms of $g(r)$, despite being strictly 2D and not including finite size effects, spatial inhomogeneities nor dissipative effects.

4. Conclusions

Despite its apparent simplicity, the system examined allows for the investigation of complex phenomena such as stationary states in the presence of agitation gradients, the effects of boundary conditions and, perhaps most importantly, polydispersity effects. An important feature observed is that granular collapse results in a locally highly packed system in some respects reminiscent of globally highly packed states.

The good agreement between experiment and polydisperse, strictly 2D MC results strongly suggests that the polydispersity is far more important than the precise shape of the size distribution, even for clearly non-trivial distributions such as those of the systems used for the present study. This is an important result given the complicated nature of many experimental size distributions and the relatively limited information in the literature regarding polydisperse quasi-2D experimental systems.

Future work will focus on gaining a better understanding of the systems studied and on extending our methods to other confined systems. In addition, we will seek to compare dynamic quantities from our experiments with results in the literature, such as the work of Watanabe and Tanaka [22].

Acknowledgements

The authors acknowledge support from Red Temática de la Materia Condensada Blanda (CONACYT) and valuable discussions with A. Trokhymchuk. AH acknowledges funding from CONACYT (project number 152431), and RS acknowledges separate support from CONACYT (Retención 174462).

1. P. M. Reis, R. A. Ingale, and M. D. Shattuck, *Phys. Rev. Lett.* **98** (2007) 188301.
2. F. Pacheco-Vázquez, G. A. Caballero-Robledo, and J. C. Ruiz-Suárez, *Phys. Rev. Lett.* **102** (2009) 170601.
3. A. Huerta, D. Henderson, and A. Trokhymchuk, *Phys. Rev. E* **74** (2006) 061106.
4. M. P. Allen and D. J. Tildesley, *Computer Simulation of Liquids* (Oxford University Press Inc., New York, USA, 1989), pp. 54–57.
5. J. Santana-Solano and J. L. Arauz-Lara, *Phys. Rev. Lett.* **87** (2001) 038302.
6. J. Santana-Solano and J. L. Arauz-Lara, *Phys. Rev. E* **65** (2002) 021406.
7. W. Wang, Z. amd Qi, Y. Peng, A. M. Alsayed, Y. Chen, P. Tong, and Y. Han, *J. Chem. Phys.* **134** (2011) 034506.
8. Z. Wang, A. M. Alsayed, A. G. Yodh, and Y. Han, *J. Chem. Phys.* **132** (2010) 154501.
9. J. Tobochnik, *Phys. Rev. E* **60** (1999) 7137.
10. P. N. Pusey and W. van Megen, *J. Chem. Phys.* **80** (1984) 3513.
11. C. Walther, S. Büchner, M. Filella, and V. Chanudet, *J. Colloid Interface Sci.* **301** (2006) 532.
12. M. Fasolo and P. Sollich, *J. Phys.: Condens. Matter* **17** (2005) 797.
13. H. Acuña-Campa, M. D. Carbajal-Tinoco, J. L. Arauz-Lara, and M. Medina-Noyola, *Phys. Rev. Lett.* **80** (1998) 5802.
14. G. Gradenigo, A. Sarracino, D. Villamaina, and A. Puglisi, *Europhys. Lett.* **96** (2011) 14004.
15. I. F. Sbalzarini and P. Koumoutsakos, *J. Struct. Biol.* **151** (2005) 182.
16. C. H. Mak, *Phys. Rev. E* **73** (2006) 065104.

17. A. Huerta, V. Carrasco-Fadanelli, and A. Trokhymchuk, *Condens. Matter Phys.* **15** (2012) 43604.

18. S. Miller and S. Luding, *Phys. Rev. E* **69** (2004) 031305.

19. L. Santen and W. Krauth, arXiv:condmat/ (2001) 0107459.

20. T. Kawasaki, T. Araki, and H. Tanaka, *Phys. Rev. Lett.* **99** (2007) 215701.

21. Z. Zhang *et al*., *Nature* **459** (2009) 230.

22. K. Watanabe and H. Tanaka, *Phys. Rev. Lett.* **100** (2008) 158002.